Wave-maker Stroke Design and Wave-decay Methods in Numerical Wave Tank Study

Tsung-Lung Liu [1] and Chun-Cheng Lin[2*]

[1] *Department of Power Vehicle and Systems Engineering, CCIT, National Defense University*
[2] *School of Defense Science, CCIT, National Defense University*

ABSTRACT

The numerical wave tank (NWT) can be considered as the ocean engineering research tool that requires the least manpower and material resources. The numerical wave tank can be used to simulate the motion of ocean wave and marine vehicle or to assist harbor design. However, the most crucial techniques of the NWT are the achievement of numerical accuracy and the treatment of reflection wave from the boundary of the computational domain. Therefore, this study employs the finite volume method (FVM), the dynamic mesh technique (DMT), the volume of fluid (VOF) model, and the wave damping zone skill to construct a NWT so as to study the physical behavior of numerical wave. Additionally, the experimental design methods are then used to investigate whether alteration of the stroke range of the wave maker would improve numerical wave quality. The results clearly show that the numerical methods provided in the present research can effectively decrease the reflection wave and enhance the accuracy of NWT.

Keywords: numerical wave tank, wave-maker, dynamic mesh, VOF model

數值波浪水槽造波器衝程設計及消波技術之研究

劉宗龍[1]　林俊成[2*]

[1]國防大學理工學院動力及系統工程學系
[2]國防大學理工學院國防科學研究所

摘　　要

數值波浪水槽的開發可謂最節約人力及物力資源的海洋工程研究，透過數值波浪水槽可模擬各種海洋波浪、船舶載具及港灣工程設計等；然而，數值波浪水槽的設計最重要的就是下游端的消波處理及數值波浪準確度，因此，本研究將採用有限體積法、動態網格、自由液面 VOF 模型及邊界波消波等數值技術構建數值波浪水槽並探討數值波浪之物理行為；另一方面，將依據實驗設計法的研究成果，探討改變造波器衝程的範圍，是否能有效改善數值波浪的品質特性。最後，本論文透過一連串模擬結果的探討及分析，將清楚呈現本研究所採的數值波浪水槽模擬技術將可有效抑制計算域邊界反射波之生成，並提昇數值波浪的計算準確度。

關鍵詞：數值波浪水槽，造波器，動態網格，VOF模型

文稿收件日期 100.7.20;文稿修正後接受日期 101.3.1; *通訊作者
Manuscript received July 20, 2011; revised March 3, 2012; * Corresponding author

Ⅰ. INTRODUCTION

Waves occur in all sizes and forms, depending on pressure forces, gravitational forces, surface tension, winds, and other factors. The study of waves can be distinguished experimental measured study from numerical simulations study. In more recent years, researchers have used various types of equipment to measure wave motion. Examples include wave pressure gauges, wave height gauges, and so on. These wave gauges are often installed on harbor and ocean observation stations, and provide ocean wave information to fishing boats and cargo ships. The requirements of wave gauge include precision, water resistance, and corrosion prevention. However, the technical development of wave gauges is mostly limited by cost, life cycle, and uncontrollable factors. Precise wave profile measurement requires long-term observation and measurements. Although these methods collect the wave information more directly, they may result in human and materials overloading. Hence, this study will try to develop a convenient numerical method for water wave generation and measurement of their characteristics. In this research a numerical piston-type wave-maker has been created. It can be employed to generate waves in a numerical wave tank (NWT), and then used a robust design method to improve the precision of the numerical wave. However, mathematical equations and physical models have difficulty explaining wave motion fully.

A brief review of the development of wave theory includes the following points: Early theorization of wave mechanic can be traced back to Laplace's theory in the eighteenth century. Subsequent theories offered a better theoretical basis for wave mechanics: Linear Wave/Small Amplitude Wave theories by Airy in 1845, Higher Order/Finite Amplitude Wave theories by Stokes in 1847, Long Wave/Solitary Wave theories by Boussinesq in 1872, Limiting Wave Heights theory by Michell in 1893 and McCowan in 1894, and Conoidal Wave theory by Korteweg and de Vires in 1895. These theories are applicable to various wave-steepness (H/λ) and height to depth ratios (H/h), and can calculate the wave motion more efficiently [1]. After World War Ⅱ, scientist began applying these wave theories to scientific, industrial, military, and renewable activities. However, many factors limit the application of free-surface simulation to NWT research. For example, it is necessary to assume that the water fluid is irrotational, and inviscid flow, and then simplify the water wave motion to be governed by the Laplace equation. In opposition to the Laplace equation, to capture the real physics of water wave, this study applies Navier-Stokes equation as the governing equation. This equation consists of non-linear terms, making it very difficult to calculate with mathematical methods [2].

Except for the study of numerical accuracy on water wave computation, NWT research has focused considerably on wave-decay methods for reflection wave in recent years. Hence, this study will develop an efficient wave decay method that ensures the quality of numerical wave profiles and prevents the wave reflection from the computational domain boundary. Regarding the treatment of reflection wave, there are three main methods which include the Sommerfeld radiation boundary condition, extension grids, and sponge layer technique. The following are examples of wave decay methods: Buchmann et al. (1998) [3] used a piston-type wave-maker to generate second-order Stokes waves in a NWT, and used a sponge layer to reduce the wave-reflection in the NWT downstream. They found the difference range of the Froude number and wave-steepness when $kh=ka=1$. They also applied the second-order Strokes wave theory by $kH \leqq 0.0708$. Kwon et al. (2003) [4] applied numerical simulation methods to study wave motion, and set the wave length/wave height to be 40 cm/3 cm. They also used a downstream wave absorber to reduce the wave reflection. They used a wave absorber with length × width × height dimensions of 0.4 m × 0.3 m × 50 mm, and noted maximum incident wave height suppression at the rate of 78%. Koo et al. (2004) [5] used a 2D NWT to simulate the fully non-linear wave motion, and designed a sponge layer as long as 2λ in the NWT downstream. They simulated two types of wave heights (1 cm and 7 cm), and discussed the swaying, heaving, and rolling of float-bodies on the free-surface. When the float-body motions are large near the resonance area, the body nonlinearity plays a much more important role in

float-body motion calculations than the free-surface nonlinearity. However, when drift forces are concerned, the free-surface nonlinearity is more important than float-body nonlinearity. Zhang et al. (2006) [6] used a Mixed Eulerian-Lagrangian formulation to generate the second-order Stokes waves, and specified the wavelength, period, and wave height as 1 m, 0.8005 s, and 0.04 m, respectively. They also used a damping zone as long as 2λ in the downstream of NWT. Their results for the linear, nonlinear, and solitary wave simulations were in good agreement with experimental or analytical solutions. Koo et al. (2006) [7] used potential flow theory to research NWT 2D fully nonlinear waves. They used a wedge-shape wave-maker to generate waves. The 2D NWT computational domain was defined as length = 4λ (including 2λ as a downstream damping zone). They used 20 or 60 nodes on free-surface per wavelength. The results of fully nonlinear designed waves ($H/\lambda \geqq 1/11$) were successfully generated with sufficient accuracy by the present NWT.

Based on wave theory and numerical simulation methods, this study applies the finite volume method (FVM), computational fluid dynamics (CFD), and volume of fraction (VOF) schemes to simulate the wave motions in a 2D NWT. There are two main goals in this research: (1) This study ascertains the effect of using extension conformal and non-conformal meshes to replace the radiation boundary condition in a NWT downstream. This study compares these two types of meshes to ensure the wave-reflection does not significantly influence the computational domain. (2) In view of the preceding Taguchi design of experiment (DOE) results, this study shows that the stroke of a piston-type wave-maker has a significant effect on the quality of the designed waves. Hence, the stroke was defined as a controllable factor in this study, and it had been adjusted to evaluate its influence on wave modulation.

This study compares these simulation results with previous research on the generation of designed waves, and demonstrates the practicality of the proposed methodology through a case study.

Ⅱ. RESEARCH METHODS

2.1 Theoretical Fundamental

The gravity surface wave considered in this study is propagating in the real viscid water fluid. Therefore, the wave motion can be modeled using the Reynolds-averaged Navier-Stokes with a $k-\varepsilon$ turbulence closure. Equations (1) and (2) determine the velocity in the *x*-direction and *z*-direction, respectively:

$$\frac{\partial u}{\partial t}+u\frac{\partial u}{\partial x}+w\frac{\partial u}{\partial z}=-\frac{1}{\rho}\frac{\partial p}{\partial x}+\nu\left(\frac{\partial^2 u}{\partial x^2}+\frac{\partial^2 u}{\partial z^2}\right) \quad (1)$$

$$\frac{\partial w}{\partial t}+u\frac{\partial w}{\partial x}+w\frac{\partial w}{\partial z}=-\frac{1}{\rho}\frac{\partial p}{\partial z}+\nu\left(\frac{\partial^2 w}{\partial x^2}+\frac{\partial^2 w}{\partial z^2}\right)-g \quad (2)$$

where u denotes the velocity in the *x*-direction, w denotes the velocity in the *z*-direction, P is the pressure, g is the acceleration of gravity, ρ is the density of liquid, and v is the kinematic viscous coefficient. This study employs a piston-type wave-maker to generate regular waves. Equations (3) and (4) define the motion of the wave-maker mentioned above. The equations are suitable for shallow water because the wave parameter kh value is less than $\pi/10$.

$$X(t)=\frac{S}{2}\times\sin\omega t \quad (3)$$

$$U(t)=\frac{S}{2}\times\omega\times\cos\omega t \quad (4)$$

$$\omega^2=gk_p\tanh k_p h \quad (5)$$

$$\left(\frac{H}{S}\right)_{piston}=\frac{2\left(\cosh 2k_p h-1\right)}{\sinh 2k_p h+2k_p h} \quad (6)$$

In Eq. (3) to (6), the terms X, U, and S represent the horizontal displacement, velocity, and stroke of the wave-maker, respectively. The term ω is the frequency of the wave-maker, H is the wave height, k_p is the wave number, and h denotes the water depth.

Previous studies presented relatively few numerical simulations of wave generation. However, the range of wave height is almost between 2 and 20 cm. Because of the theoretical basis for this study and the status of the field as reviewed above, it is necessary to satisfy the piston wave-maker conditions of $kh \leqq \pi/10$. Previous research on wave motion reveals the

following values: water depth (h), wave number (k), wave-maker frequency (ω), and period (T). This study adopts these parameters for NWT study.

2.2 Numerical Methods

To build a numerical wave tank and simulate a real ocean wave, three kinds of commercial software were used to do the pre- and post-processing works for the CFD simulation of NWT. The CAD software Rhino was first applied to contrive the configuration of NWT. The length and height of the NWT are 250m and 12m respectively. Meanwhile, the water depth of the NWT is 2m for all case studies in this research. After taking advantage of the CAD software for geometric design of NWT, GRIDGEN commercial software was then used to construct the structured and unstructured meshes for the computational domain of NWT. However, the grids on the free-surface should be refined to resolve the correct wave profile. In the unstructured mesh zone, a user-define-function (UDF) provided by a flow solver software FLUENT 6.2 was programmed to simulate the piston-type wave-maker motion. The UDF program was used to control the stroke moving range and velocity of the wave-maker. While the wave-maker moved, the grids nearby it would be remeshed automatically to keep the grid quality in the unstructured mesh zone. In the present research, it can be obviously found that the wave profile shown in structured mesh zone is better than unstructured mesh zone. Therefore, the structured mesh zone was constructed followed by the unstructured grid region. The NWT boundary conditions were defined as follows: the upstream side applied with piston-type wave-maker to simulate wave generation, the downstream side applied with the pressure outlet and grid allocation (conformal grids and non-conformal grids) to avoid wave reflection, and the upper and bottom sides applied with symmetry and wall boundary conditions respectively to simulate the ocean environment. The FLUENT 6.2 commercial software was used to reveal the flow physics in the NWT. The numerical methods embedded in the FLUENT consist of the following: finite volume method/dynamics mesh/VOF, and k-ε scheme. Table 1 presents the schematic setup in the FLUENT solver for the flow computation of NWT. The volume of fraction (VOF) scheme was adopted to efficiently deal with free-surface. The free surface was determined by the following equation :

$$\alpha(x,z,t)=\begin{cases}1 \text{ defined as water}\\ 0 \text{ defined as air}\end{cases} \tag{7}$$

$$\frac{\partial \alpha}{\partial t}+\nabla\cdot\left(\bar{u}\alpha\right)=0 \tag{8}$$

The value of α is between null and unity. When α value in a computational mesh is equal to zero, the fluid material in this mesh is air. On the contrary, the computational domain is occupied by water as the value of α is equal to one. Meanwhile, when the computational domain has the α value between 0 and 1, this region will be filled with the air-water mixing material. Hence, this study defines the free-surface as α = 0.5. The post-processor software Tecplot was used to measure the wavelength and wave height of the numerical wave. The numerical results were then compared with analytic solution. Fig. 1 presents the dynamic motion of the piston-type wave-maker. As shown in Fig. 1, the FLUENT dynamic mesh module was used to remesh the grids in the unstructured mesh zone according to the dynamic movement of the wave-maker. Then the movement of wave-maker will generate the desire wave propagating in the structured mesh zone.

Table 1. Schematic flow field setup

FLUENT	Numerical Methods
Solver	Segregated
Multiphase	VOF
Viscous Model	k - ε
Press-Velocity Coupling	SIMPLE
Pressure	PRESTO
Momentum	Second Order Upwind
Volume Fraction	Second Order Upwind

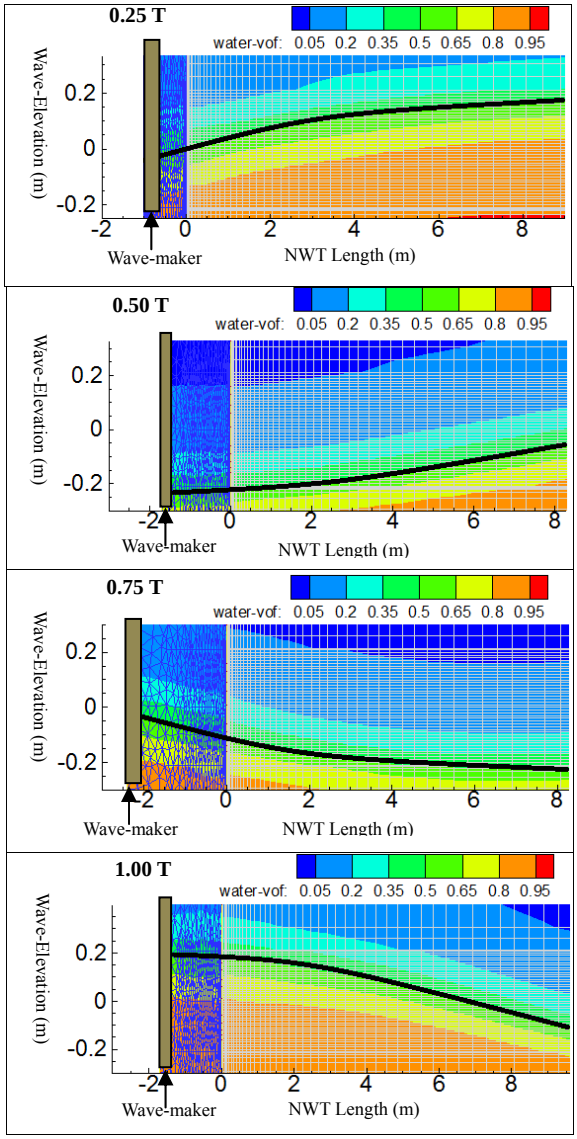

Fig. 1. The dynamic mesh motion of the piston-type wave-maker

2.3 Test of Grid Quality

It is true that the grid quality of the computational domain will strongly affect the accuracy of numerical results. However, to date, there has been relatively little research conducted on the relationship between the use of grid numbers and the accuracy of numerical wave simulation. Thus the influence of grid quality on accuracy of the numerical wave generated in NWT would be investigated in the present study. What guarantee the numerical solution will be close to the exact solution of the governing equation? Generally numerical solution converges to a unique solution with grid refinement, but it is very hard to prove. To that end, two test cases which concerning the usage of grid points in wave length and wave height directions have been studied. The numerical results obtained with different grid numbers will be compared each other.

The first test case is based on previous research results (N_H=61) [8], and allocates the grid numbers N_λ=151 and N_λ=301 in each wavelength respectively for the comparison of influence of grid point usage in wavelength direction. Shown as Fig. 2 and Table 2, it can be seen that the wave profiles of both numerical simulations with 151 and 301 grid points in each wavelength are almost the same at the sixth period of wave-maker motion. The use of coarse grid could act like a low-pass filter. It filters out the high frequency components. The high frequency waves would supposedly damp out in a coarse grid region. However, these results show that N_λ=151 could capture the high frequency wave property. It not only provides the enough accuracy, but also saves one third of the computation time.

Table 2. The comparison of grid allocation on wave-length

period (T)	λ-grid	1st-λ (m)	2nd-λ (m)	3rd-λ (m)	4th-λ (m)	calculate-time	total-grids
6T	301	40.7909	40.7911	40.791	38.159	48 hrs-30 mins	150750
	151	40.7909	40.7911	40.791	37.72	30 hrs-48 mins	119930

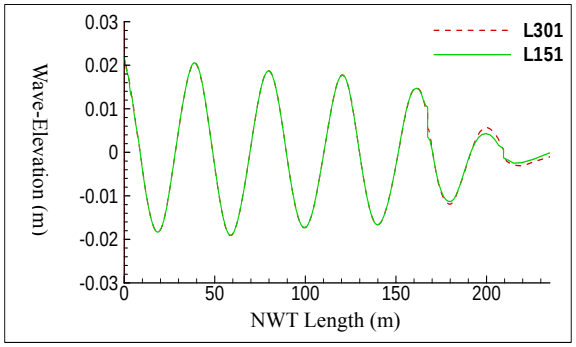

Fig. 2. The comparison of wave profiles with N_λ=301 and N_λ=151 at wave period =6T.

The second case is also based on previous results (N_λ=151) [8], and allocates different values of grid point N_H=61 and N_H=121 in wave elevation region for the comparison of influence of grid point usage in wave height direction. Table 3 and Fig. 3 shows the comparison results of wave height obtained with different values of N_H at wave period equal to 6T. As can be clearly

seen in Table 3 and Fig. 3, the difference between the two wave profiles is very small. As mentioned in previous discussion, the more grid points we use, the better results we could obtain. These results indicate that the N_H=61 could provide enough accuracy for wave height computation and saves half the computation time.

Table 3. The comparison of grid allocation on wave-height

period (T)	H-grid	1st-H (m)	2nd-H (m)	3rd-H (m)	4th-H (m)	calculate-time	total-grids
6T	121	0.0386	0.0348	0.0318	0.0291	60 hrs-18 mins	192130
	61	0.0388	0.0377	0.0350	0.0314	30 hrs-48 mins	119930

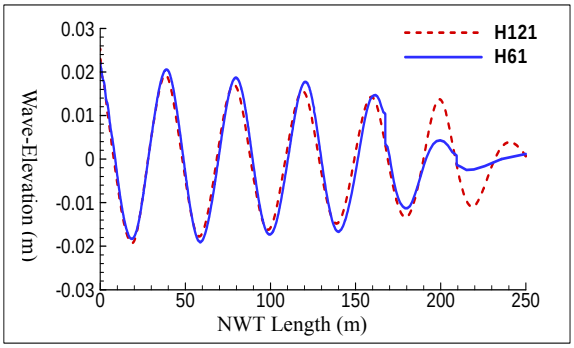

Fig. 3. The comparison of wave profiles with N_H=121 and N_H=61 at wave period =6T.

Among the case studies, the results of the present research suggest the followings: the values of grid point N_λ=151 and N_H=61 could be enough to capture the profile of designed waves, and are therefore used in this study to construct the measure zone of the 2D NWT.

Ⅲ. WAVE-DAMPING METHODS

An ocean wave is an incompressible flow. Therefore, the NWT must own the specific performance to dissipate energy of reflection wave bouncing back from the downstream boundary. Without effective wave-amplitude reduction methods, the profiles of progressive waves in measure zone are significantly influenced by reflection waves. In recent years, wave-damping methods have attracted considerable interest in NWT research. This highlights the need to develop a robust wave amplitude reduction method, and ensure the quality of numerical wave simulation in measure zone of NWT. Regarding the treatment of reflective waves, there are three main methods were posed: the application of Sommerfeld radiation BC, elongation of computational domain, and usage of sponge layer. The proposed method constructs an elongation computational domain as a wave-damping region to efficiently reduce wave reflection. It has been shown that 3-times wave length space is enough in the wave-damping region to prevent reflective wave from the computational boundary.

The length of the 2-D NWT is 6 times the wave length (6λ) in this study. To apply the method mentioned above, the computational domain has been divided into two regions which can be named as measure and damping zones respectively. The length of measure and damping zones are all 3 times the wave length. Two cases with different kinds of grid allocation were conducted to address this wave-damping issue. The first and second cases deployed the conformal and non-conformal grids in damping zone shown as Fig. 4 and Fig. 6 respectively.

3.1 Usage of Conformal Grids in Damping Zone

In the first case computation, the simulation time ranged from 0 to 12 periods of wave-maker motion. Fig. 5 shows a schematic of wave propagation at different time steps. The results of this case study reveal that the average wave height in the computational domain increases with flow time. This shows that the reflected wave in the damping zone is significant. In this case, after the fifth period of wave-maker motion the wave reflection rate varied from 0.70% to 21.78% during simulation time 5T - 12T shown as table 4. The numerical results reveal that the usage of conformal grid does not help much to accomplish the goal of wave-amplitude reduction.

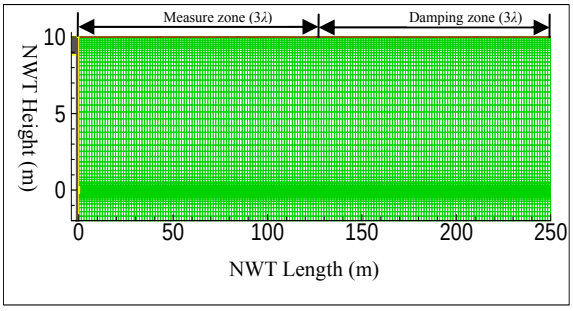

Fig. 4. Conformal grid allocation in 2D NWT

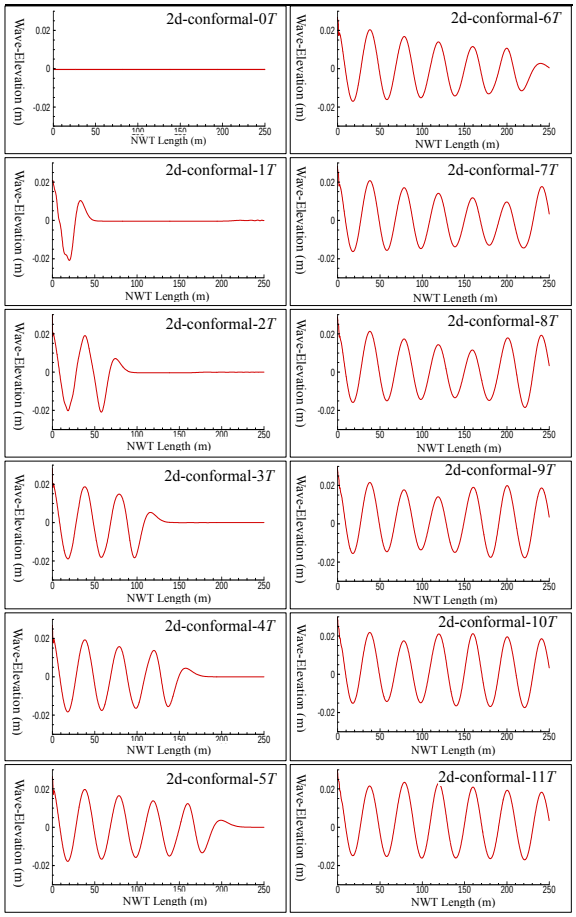

Fig. 5. Wave profile variation from 0 to 11*T* for conformal grid case

Table 4. Wave height statistics for conformal grid case at simulation time 5*T*-12*T*

2d-conformal-grid							
	Observation Zone (m)			Damping Zone (m)		Observative Zone Ave. *H* (m)	*H*-reflective rate
Time	*H1*	*H2*	*H3*	*H4*	*H5*		
5T	0.0375	0.0331	0.0295	0.0273	0.0170	0.0334	—
6T	0.0373	0.0329	0.0292	0.0258	0.0238	0.0331	0.70%
7T	0.0369	0.0326	0.0288	0.0256	0.0226	0.0328	1.80%
8T	0.0371	0.0323	0.0286	0.0248	0.0327	0.0327	2.10%
9T	0.0371	0.0323	0.0277	0.034	0.0374	0.0324	3.00%
10T	0.0369	0.0316	0.0358	0.0377	0.0363	0.0348	4.20%
11T	0.0363	0.0386	0.039	0.0369	0.0355	0.0380	13.79%
12T	0.0425	0.0410	0.0384	0.0364	0.0352	0.0406	21.78%

3.2 Usage of Non-conformal Grids in Damping Zone

To reduce the wave height of reflective wave effectively, the second test case embedded with the non-conformal grids in the damping zone. The dimension of the damping zone is three times as long as the wave length. Meanwhile, this zone is divided into three equal sections. Along the wave propagation direction the arrangement of N_λ value in the three sections is 76, 25, 13 respectively which correspond to 1/2, 1/6, and 1/12 of N_λ = 151 used in measure zone. Moreover, to enhance the wave damping effect, the grid points in the wave elevation direction are also reduced in such artificial wave-damping region. The arrangement of the value of grid points used in wave elevation region in such three sections is 31, 15, 8 respectively which correspond to 1/2, 1/4, and 1/8 of N_H = 61 used in measure zone. The distribution of non-conformal grids in the wave-damping area can be seen in Fig. 6.

To test the performance of the damping zone consisting of non-conformal grids, the simulation was carried out 12 period of wave-maker motion for the present study. Fig. 7 shows a schematic of wave propagation process. Table 5 presents wave height statistics for non-conformal grid test case at simulation time 5*T*-12*T*. In Table 5, *H1, H2, H3, H4* and *H5* denote the values of wave height of the first, second, third, fourth, and fifth waves counted from the wave maker respectively. These results show that the average wave height in the computational domain ranged between 0.0371 and 0.0379 meter. Mentioned as previous paragraph, the 2D NWT is six times the length of wave length so as the wave reflection phenomena can be observed after the fifth period of wave-maker motion. However, from this case study we could clear to know about the wave reflection rate between 0.36% and 1.70%. Table 5 presents the wave height statistics from 5*T* - 12*T* using non-conformal grid in damping zone. It clearly indicates that the usage of non-conformal grid is better than that of conformal grid for dissipation of reflective waves.

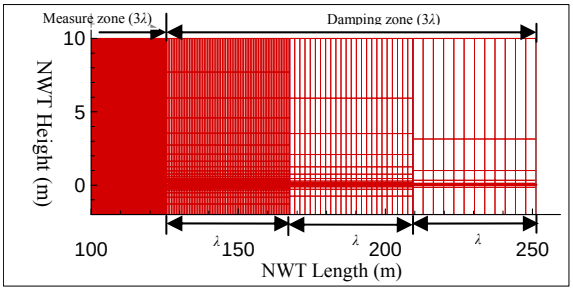

Fig. 6. Non-conformal grid allocation in 2D NWT

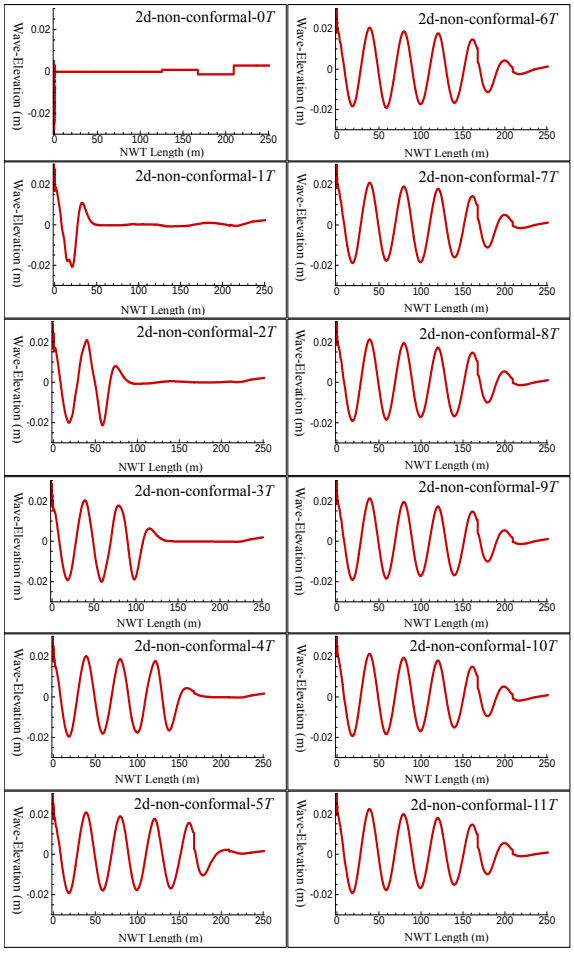

Fig. 7. Wave-profile variation from 0 to 11*T* for non-conformal grid case

Table 5. Wave height statistics for non-conformal grid case at simulation time 5*T*-12*T*

2d-non-conformal-grid							
	Measure Zone (m)			Damping Zone (m)		Observative Zone Ave.	*H*-reflective rate
Time	*H1*	*H2*	*H3*	*H4*	*H5*	*H* (m)	
5T	0.0398	0.0367	0.0352	0.0323	0.0126	0.0372	—
6T	0.0388	0.0375	0.035	0.0313	0.0156	0.0371	0.36%
7T	0.0396	0.0367	0.0364	0.0302	0.0161	0.0376	0.90%
8T	0.0402	0.0378	0.0344	0.0315	0.0154	0.0375	0.63%
9T	0.0407	0.0373	0.0353	0.0296	0.0159	0.0378	1.43%
10T	0.0406	0.0378	0.0348	0.0299	0.0145	0.0377	1.34%
11T	0.0414	0.0375	0.0347	0.0296	0.0115	0.0379	1.70%
12T	0.0404	0.0377	0.0345	0.0299	0.0149	0.0375	0.81%

3.3 Validation of Wave-damping Effect

As mentioned previously, the length of the present NWT is 250 m. To ensure complete analysis in this study, the period of wave-maker motion was increased to 30*T*, and the rate of wave reflection was analyzed. One point locating at the position *x*=40m of the computational domain was checked to investigate the influence of grid allocation on the profile of progressive waves. Fig. 8 compares the wave profiles which were obtained from two different kinds of grid deployment in daming zone from simulation time 0-30*T*. Meanwhile, Fig. 9 shows the comparison result of normalized wave profiles manipulated from Fig. 8. These results show that the use of non-conformal grids in the damping zone achieved more efficient for wave damping than conformal grids did. In addition, the non-conformal grids revealed no significant wave reflection, and did not influence the wave profiles in the computational domain. In conclusion, Three times the length of wavelegth of non-conformal damping zone can help avoid wave reflection problem and eliminate the disturbance of reflective wave in measure zone.

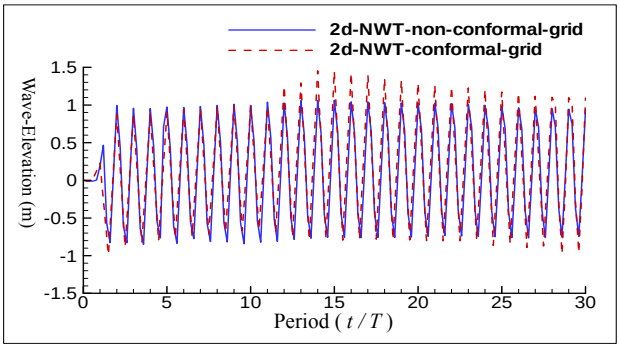

Fig. 8. Comparison of wave profiles given with conformal and non-conformal grids in damping zone/measure position *x*=40m

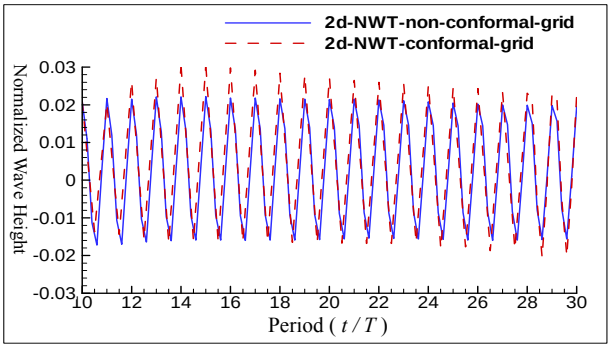

Fig. 9. Comparison of normalized wave profiles given with conformal and non-conformal grids in damping zone/measure position *x*=40m

Ⅳ. STROKE of PISTON-TYPE WAVE-MAKER DESIGN

Liu and Lin (2011) [8] proposed a robust

design method for 2D-NWT based on the Taguchi Method. They also used analysis of variance (ANOVA) to detect significant differences among control factors. Table 6 presents the results of ANOVA for the average wave height error rate. These ANOVA results indicate significant effects on these four control factors, and insignificant interaction effects for all control factors. Hence, this case study shows that the hypothesis is accepted at a significant level of 95% for all control factors. The optimum designed factors for error of average wave height was 12.98%.

Table 6. ANOVA of designed wave height average error rate [8]

ANOVA of S/N ratio					
Factor	DOF	F	$F_{0.05}$	Contribution (%)	P-Test
A	2	30.8022	3.5546	18.87%	1.55E-06
B	2	20.3771	3.5546	12.27%	2.38E-05
C	2	75.7159	3.5546	47.31%	1.72E-09
D	2	22.0464	3.5546	13.33%	1.45E-05
A×B	Pooled			—	—
A×C	Pooled			—	—
B×C	Pooled			—	—
Error	18	—		8.23%	
Sum	26			100%	

This study may lead to a better understanding of how to improve wave height reliability in NWT. The results above show a clear and strong relationship between kh and H/λ. These two control factors provide 60.64% contribution for wave height quality characteristic in 2D-NWT. According to the results, kh = 0.3 and H/λ = 1/100 could achieve superior quality for the computation of numerical waves. A piston-type wave-maker must satisfy the condition of shallow water wave generation theory ($H/S = kh$). When kh = 0.3 ($kh \leqq \pi/10$), the stroke (S) of the wave-maker is strongly and positively correlated with designed wave height (H). In the other words, it is necessary to consider the designed wave height value (H) first in a NWT. Then, wave-maker theory can be used to determine the stroke range. These results reveal that the H/λ value appears to be an important variance and less the better. Hence, a reasonable stroke range leads to better quality in the designed wave.

In light of these results, this study applies Taguchi-Method DOE optimum factorial design (grid numbers of per wave length N_λ = 151, grid numbers of per wave height N_H = 61, kh = 0.3 and H/λ = 1/100). This study proposes the following four different stroke range methods. The original stroke Stroke-1 was set at ($S_{1.0}$ = 1.396 m), and Stroke-2 ($S_{0.5}$ = 0.698m) was half of $S_{1.0}$, Stroke-3 ($S_{0.25}$ = 0.349m) was 1/4 of $S_{1.0}$, and Stroke-4 ($S_{0.1}$ = 0.1396m) was 1/10 of $S_{1.0}$. These four different strokes made it possible to compare and discuss the quality characteristic of wave height. To provide a detailed understanding of the relationship between stroke ranges and wave quality, this study measures the first 5 waves. The error rate of wave height (E_H) and error rate of wave length (E_λ) served as smaller-the-better quality characteristics. The analytic solution of wave height and wave length was denoted as H_a and λ_a. Equations (9) and (10) compare the error rates of the designed wave. The E_H and E_λ were defined as smaller-the-better quality characteristics.

$$E_H = \frac{H_i - H_a}{H_a} \times 100\% \tag{9}$$

$$E_\lambda = \frac{\lambda_i - \lambda_a}{\lambda_a} \times 100\% \tag{10}$$

4.1 Stroke-1

Stroke-1 ($S_{1.0}$) was the original stroke, and was set at $S_{1.0}$ = 1.3960 m. This led to the analytical solution of wave height (H_a = 0.4188 m) and wave length (λ_a = 41.8879 m). This study set the simulation time from 0 to 6 periods of wave-maker motion. Fig. 10 shows the wave profiles obtained from numerical simulation and analytic computation. It highlights larger differences between the two approaches. Table 7 summarizes the error rate of numerical wave length and wave heig NWT Length (m) lts show that the average numerical wave height was 0.3164 m, and error rate of H was 24.45%. The average numerical wave length was equal to 41.2960 m, and error rate of λ was 1.76%.

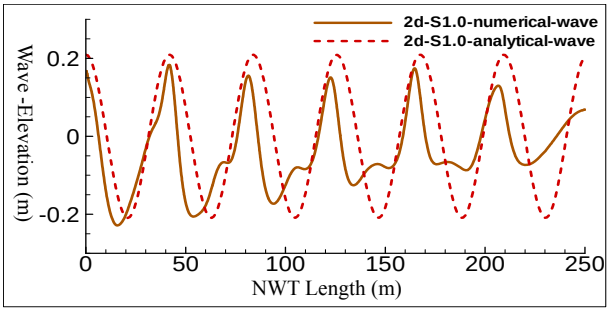

Fig. 10. Comparisons of numerical and analytic

wave-profiles for stroke value $S_{1.0}$

Table 7. Error rate of numerical wave length and wave height for stroke value $S_{1.0}$

Stroke-1	$S_{1.0}$=1.3960 (m)		H_a=0.4188 (m)		λa=41.8879 (m)	
	H1	*H2*	*H3*	*H4*	*H5*	Ave.-*H*
	0.4087	0.3607	0.3205	0.2756	0.2165	0.3164
H-Error rate	2.41%	13.87%	23.47%	34.19%	48.30%	24.45%
	λ1	*λ2*	*λ3*	*λ4*	*λ5*	Ave.-*λ*
	41.2696	39.5422	41.7092	41.7090	42.2500	41.2960
λ-Error rate	1.48%	5.60%	0.43%	0.43%	0.86%	1.76%

4.2 Stroke-2

Stroke-2 ($S_{0.5}$) was half of the original stroke, and was set at $S_{0.5}$ = 0.6980 m. This led to the analytic solution of wave height (H_a = 0.2094 m) and wave length (λ_a = 41.8879 m). Same as the previous study, the simulation for the current study endures also from 0 to 6 periods of wave-maker motion. Fig. 11 shows the comparison results between numerical and analytic computation. Table 8 summarizes the error rate of numerical wave length and wave height. These results show that the average numerical wave height was equal to 0.1927 m, and error rate of H was 8.87%. The average numerical wave length was equal to 41.2496 m, and the error rate of λ was 1.95%.

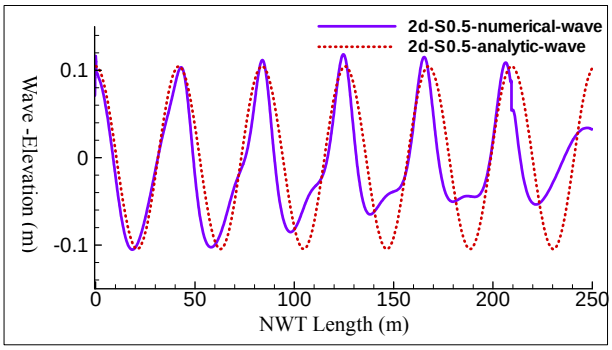

Fig.11. Comparisons of numerical and analytic wave-profiles for stroke value $S_{0.5}$

Table 8. Error rate of numerical wave length and wave height for stroke value $S_{0.5}$

Stroke-2	$S_{0.5}$=0.6980 (m)		H_a=0.2094 (m)		λa=41.8879 (m)	
	H1	*H2*	*H3*	*H4*	*H5*	Ave.-*H*
	0.2080	0.2140	0.2033	0.1789	0.1591	0.1927
H-Error rate	0.67%	2.20%	2.91%	14.57%	24.02%	8.87%
	λ1	*λ2*	*λ3*	*λ4*	*λ5*	Ave.-*λ*
	42.3352	41.2496	41.2500	40.7070	40.7060	41.2496
λ-Error rate	1.07%	1.52%	1.52%	2.82%	2.82%	1.95%

4.3 Stroke-3

Stroke-3 ($S_{0.25}$) was 1/4 the original stroke, and was set at $S_{0.25}$ = 0.3490 m. This led to the analytic solution of wave height (H_a = 0.1047m) and wave length (λ_a = 41.8879m). The simulation for the present study is from 0 to 6 periods of wave-maker motion. Fig. 12 shows the numerical and analytic wave-profiles comparison diagram. Compared with other case studies, it displays smaller differences between the two approaches. Table 9 summarizes the error rate of numerical wave length and wave height. These results show that the average numerical wave height was equal to 0.0955 m, and error rate of H was 8.83%. The average of numerical wave length was equal to 41.1878 m, and error rate of λ was 2.12%.

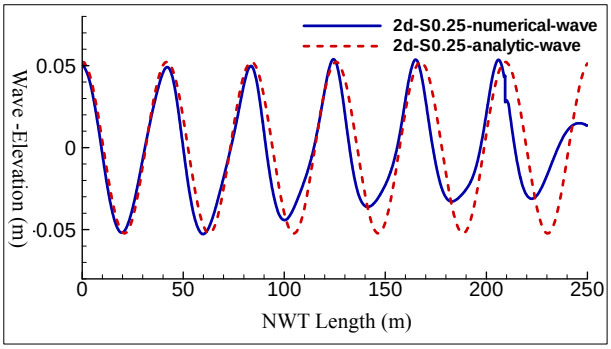

Fig. 12. Comparisons of numerical and analytic wave-profiles for stroke value $S_{0.25}$

Table 9. Error rate of numerical wave length and wave height for stroke value $S_{0.25}$

Stroke-3	$S_{0.25}$=0.349 (m)		H_a=0.1047 (m)		λa=41.8879 (m)	
	H1	*H2*	*H3*	*H4*	*H5*	Ave.-*H*
	0.1009	0.1024	0.0979	0.0898	0.0863	0.0955
H-Error rate	3.63%	2.20%	6.49%	14.23%	17.57%	8.83%
	λ1	*λ2*	*λ3*	*λ4*	*λ5*	Ave.-*λ*
	42.3529	41.1673	40.0838	41.1670	41.1680	41.1878
λ-Error rate	1.11%	1.72%	4.31%	1.72%	1.72%	2.12%

4.4 Stroke-4

Stroke-4 ($S_{0.1}$) was 1/10 the original stroke, and was set at $S_{0.1}$ = 0.1396 m. This led to the analytic solution of wave height (H_a = 0.0419m) and wave length (λ_a = 41.8879m). The simulation time for the current study is same as the previous three cases. The wave-profiles obtained from the numerical and analytic computation can be seen in Fig. 13. Though it is possible to detect differences between the two wave-profiles, theses differences do not prove very impressive from a physical point of view. In general, wave energy dissipation in a real ocean is closely related to wave propagation.

The wave energy dissipation arises from the friction of fluid particle motion and it would likely reduce the wave height. Therefore, it can be argued that the differences could arise from no contribution of viscous effect being considered for analytic wave computation. Table 10 summarizes the error rate of numerical wave length and wave height. These results show that the average of numerical wave height was equal to 0.0362 m, and error rate of H was 13.51%. The average numerical wave length was equal to 41.0614 m, and error rate of λ was 1.97%.

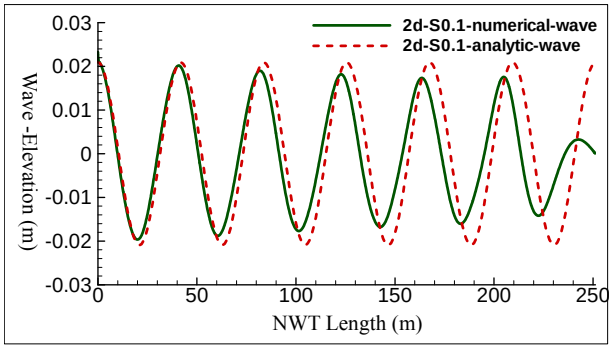

Fig. 13. Comparisons of numerical and analytic wave-profiles for stroke value $S_{0.1}$

Table 10. Error rate of numerical wave length and wave height for stroke value $S_{0.1}$

Stroke-4	$S_{0.1}$=0.1396 (m)		H_a=0.0419 (m)		λa=41.8879 (m)	
	H1	*H2*	*H3*	*H4*	*H5*	Ave.-*H*
	0.0398	0.0378	0.0359	0.0342	0.0335	0.0362
H-Error rate	5.01%	9.79%	14.32%	18.38%	20.05%	13.51%
	λ1	*λ2*	*λ3*	*λ4*	*λ5*	Ave.-*λ*
	40.7121	41.2661	41.2658	40.3280	41.7350	41.0614
λ-Error rate	2.81%	1.48%	1.49%	3.72%	0.37%	1.97%

V. RESULTS and DISCUSSION

In this study, the boundary conditions and initial conditions must satisfy wave-maker theory. Hence, there are two themes finding worth summarization: (a) the results show a striking effect of non-conformal grids on reducing of wave reflection, and (b) the results show that the stroke range has a significant effect on simulated wave quality.

1. For 2-D NWT, the usage of 3λ conformal grid allocation in the damping zone. This study discusses the dissipation efficiency of damping zone. Table 11 presents the numerical wave height and decay rate of reflection wave from 5-12T. These results show that the influences of reflection wave approximate 6.76%. The maximum wave-reflection rate occurred at 12T, and the wave height reflection rate was 21.78%. However, the quality of designed wave-profiles at 30T reveals more uncertainty and influence on the measure domain.

Table 11. Record of numerical wave height and reflection wave decay rate from 5-12T for conformal grid deployment in damping zone

2D-NWT conformal grid									
	5T	*6T*	*7T*	*8T*	*9T*	*10T*	*11T*	*12T*	Ave.
$\overline{H}$	0.0334	0.0331	0.0328	0.0327	0.0324	0.0348	0.0380	0.0406	0.0347
Reflective rate	—	0.70%	1.80%	2.10%	3.00%	4.20%	13.78%	21.78%	6.76%

2. For the case studies of non-conformal grid allocation in damping zone, table 12 presents the numerical wave height and wave-reflection decay rate from 5-12T. These results show that the average wave-reflection influence on the wave profile in measure zone is almost 1.02%. The maximum wave-reflection rate occurred in the eleventh period of wave-maker motion, and the wave height reflection rate was 1.70%. These results show that the damping effect contributed by the use of non-conformal grids is better than that of conformal grids. While performing a long period simulation such as the wave-maker motion at 30T, it can be observed that the quality of numerical wave profiles in measure zone is little influenced by the reflection wave. In other words, these results indicate that the usage of non-conformal grids in damping zone could be regarded as a good way to dissipate the reflective wave from the downstream boundary of the computational domain.

Table 12. Record of numerical wave height and reflection wave decay rate from 5-12T for non-conformal grid deployment in damping zone

2D-NWT non-conformal grid									
	5T	*6T*	*7T*	*8T*	*9T*	*10T*	*11T*	*12T*	Ave.
$\overline{H}$	0.0372	0.0371	0.0376	0.0375	0.0378	0.0377	0.0379	0.0375	0.0375
Reflective rate	—	0.36%	0.90%	0.63%	1.43%	1.34%	1.70%	0.81%	1.02%

3. Regarding the influence of stroke values on numerical wave quality, four different stroke values are tested. The numerical results indicate that the average error rate of wave length is between 1.76% and 2.12%. These

results are all less than the target of 5%, and were reasonably accepted. However, for the computation of numerical wave height, Stroke-2 ($S_{0.5}$ = 0.6980 m) / Stroke-3 ($S_{0.25}$ = 0.3490 m) and Stroke-4 ($S_{0.1}$ = 0.1396 m) led to average wave height average error ranging from 8.83% to 13.51%. These results are significantly better than the results obtained from Stroke-1. It can be seen in Table 13, Case studies for Stroke-2, Stroke-3 and Stroke-4 have achieved an improvement of 63.72%, 63.89%, and 44.74%, respectively.

Table 13. Comparisons of average error rate of numerical wave height and wave length for different stroke values

Stroke	Range	Ave. Error Rate for λ	Ave. Error Rate for H	Improvement for $S_{1.0}$
Stroke-1	$S_{1.0}$=1.3960 (m)	1.76%	24.45%	—
Stroke-2	$S_{0.5}$=0.6980 (m)	1.95%	8.87%	63.72%
Stroke-3	$S_{0.25}$=0.3490 (m)	2.12%	8.83%	63.89%
Stroke-4	$S_{0.1}$=0.1396 (m)	1.97%	13.51%	44.74%

4. The application of NWT can be regarded as a useful tool in the study of ocean engineering. Though this study has applied various numerical techniques for numerical wave generation and saves manpower and material resources focused on wave experiment. However, the piston-type wave-maker studied in the present research is just suitable for shallow wave generation. The use of such kind of wave-maker is limited by the value of kh less than $\pi/10$. In conclusion, the choice of stroke value is important for the operation of the piston-type wave-maker.

Ⅵ. CONCLUSION

The results of this study show that extended non-conformal meshes can significantly reduce wave reflection in a 2D NWT. These results were more improvement for reducing the reflection wave from the downstream. In addition, Stroke-2 and Stroke-3 achieved a greater improvement in numerical wave computation. For these two cases Stroke-2 and Stroke-3, the average error rate of first five numerical wave height are improved by 63.72% and 63.89% respectively. These results were entirely consistent with the goals of this study and illustrate a significant improvement in numerical wave generation.

This study presents the results of 2D NWT wave-reflection reduction and the effect of different strokes on numerical wave quality. The results of this study clearly support the concept of robust design. Although this study has its limitations, it can serve as a basis for future study in wave-body interaction simulation for 3D flow field computation.

SYMBOLS

a	amplitude of wave
E_H	average error rate of wave height
E_λ	average error rate of wave length
g	acceleration of gravity
h	water depth
H	wave height
$\overline{H}$	average wave height
H_a	analytical solution of wave height
H_i	wave height at specific position
k	wave number
k_p	propagation wave number
N_H	grid numbers per wave height
N_λ	grid numbers per wave length
P	pressure
S	stroke of the wave-maker
$S_{0.1}$	the one-tenth of original stroke of piston-type wave-maker
$S_{0.25}$	the quarter of original stroke of piston-type wave-maker
$S_{0.5}$	the half of original stroke of piston-type wave-maker
$S_{1.0}$	the original stroke of piston-type wave-maker
t	current time
T	wave period
U	velocity of piston-type wave-maker
u	velocity of x-direction
w	velocity of z-direction

X	position of piston-type wave-maker
x	position of x-direction
z	position of z-direction
α	parameter of VOF scheme
λ	wave length
λ_a	analytical solution of wave length
λ_i	wave length at specific position
ρ	the density of liquid
v	the kinematic viscosity of fluid
ω	the frequency of wave-maker

REFERENCES

[1] Hsu, T. W., Nearshore Hydrodynamics, Chinese Institute of Civil and Hydraulic Engineering, pp.227-238, 2003.[Chinese]

[2] Dean, R. G. and Dalrymple, R. A., Water Wave Mechanics for Engineers and Scientists, World Scientific, pp. 43-82, 170-185, 1991.

[3] Buchmann, B., Skourup, J., and Cheung, K.F., "Run-up on a structure due to second-order waves and a current in a numerical wave tank", Applied Ocean Research, Vol. 20, pp. 297-308, 1998.

[4] Kwon, S. H., Moon, W. M., and Lee, H. S., "Experimental and numerical studies on the development of a new wave absorber", Ocean Engineering, Vol. 30, pp.185-203, 2003.

[5] Koo, W. and Kim, M. H., "Freely floating-body simulation by a 2D fully nonlinear numerical wave tank", Ocean Engineering, Vol. 31, pp. 2011-2046, 2004.

[6] Zhang, X. T., Khoo, B. C., and Lou, J., "Wave propagation in a fully nonlinear numerical wave tank: A desingularized method", Ocean Engineering, Vol. 33, pp. 2310-2331, 2006.

[7] Koo, W. C. and Kim, M. H., "Numerical simulation of nonlinear wave and force generated by a wedge-shape wave maker", Ocean Engineering, Vol.33, pp.983–1006, 2006.

[8] Liu, T. L., Wu, S. J., and Lin, C. C., "Application of Experimental Design and Genetic Algorithms Methods for the Robust Design in 2D Numerical Wave Tank", Proc 21st Int Offshore Polar, ISOPE, Maui, Vol. 3, pp. 680-686.